A hybrid fuzzy logic proportional-integral-derivative and conventional on-off controller for morphing wing actuation using shape memory alloy Part 1: Morphing system mechanisms and controller architecture design

T. L. Grigorie, R. M. Botez and A. V. Popov
École de Technologie Supérieure
Montréal, Québec, Canada

M. Mamou and Y. Mébarki
National Research Council
Ottawa, Ontario, Canada

ABSTRACT

The present paper describes the design of a hybrid actuation control concept, a fuzzy logic proportional-integral-derivative plus a conventional on-off controller, for a new morphing mechanism using smart materials as actuators, which were made from shape memory alloys (SMA). The research work described here was developed for the open loop phase of a morphing wing system, whose primary goal was to reduce the wing drag by delaying the transition (from laminar to fully turbulent flows) position toward the wing trailing edge. The designed controller drives the actuation system equipped with SMA actuators to modify the flexible upper wing skin surface. The designed controller was also included, as an internal loop, in the closed loop architecture of the morphing wing system, based on the pressure information received from the flexible skin mounted pressure sensors and on the estimation of the transition location.

The controller's purposes were established following a comprehensive presentation of the morphing wing system architecture and requirements. The strong nonlinearities of the SMA actuators' characteristics and the system requirements led to the choice of a hybrid controller

Paper No. 3699(i). Manuscript received 12 February 2011,
revised version received 2 September 2011, accepted 13 October 2011.

architecture as a combination of a bi-positional on-off controller and a fuzzy logic controller (FLC). In the chosen architecture, the controller would behave as a switch between the SMA cooling and heating phases, situations where the output current is 0A or is controlled by the FLC.

In the design phase, a proportional-integral-derivative scheme was chosen for the FLC. The input-output mapping of the fuzzy model was designed, taking account of the system's error and its change in error, and a final architecture for the hybrid controller was obtained. The shapes chosen for the inputs' membership functions were *s*-function, π-function, and *z*-function, and product fuzzy inference and the center average defuzzifier were applied (Sugeno).

NOMENCLATURE

A	fuzzy set in the antecedent
	associated individual antecedent fuzzy sets of each input variable
B	fuzzy set in the antecedent
	scalar offset
dY_1, dY_2	displacements of the two control points of the flexible skin
dY_{1opt}	optimal vertical displacement of actuator 1
dY_{2opt}	optimal vertical displacement of actuator 2
dY_{1real}	real vertical displacement of actuator 1
dY_{2real}	real vertical displacement of actuator 2
e	actuation loop error
FLC	fuzzy logic controller
FP	fuzzy proportional controller
F_{aero}	aerodynamic force
F_{skin}	elastic force produced by the flexible skin
F_{spring}	elastic force of the gas spring
f	a crisp function in the consequent (a polynomial function)
$i(t)$	command variable (electrical current in the present case)
K_D	derivative gain
K_I	integral gain
K_O	change in output gain
K_P	proportional gain
k	discrete step
M	Mach number
mf	membership function
N	number of rules
q	number of inputs
Re	Reynolds number
T_D	derivative time constant
T_s	sample period
t	time
$w^i(x)$	degree of fulfillment of the antecedent, i.e., the level of firing of the ith rule
x	independent variable on the universe of discourse
x_{left}	left breakpoint
x_q	individual input variables
x_{right}	right breakpoint
$\mathbf{x}$	input vector

y output of the fuzzy model
y^i polynomial function in the consequent
Δe actuation loop change in erro
α angle-of-attack

1.0 INTRODUCTION

In the aerospace vehicle field, wing morphing refers to the ability of an aircraft wing to change shape during flight, thereby providing aerodynamic performance advantages. The wing morphing approach is referred to as the variform wing concept. In this way, a morphing wing can be considered as a wing that has the ability to either alter its shape in a continuous change along the chord or spar, or to change its shape in a drastic manner[1-3]. The highest present demand on fuel consumption has emphasised the importance of improving aerodynamic efficiency through modification of the wing geometry that can move the laminar-to-turbulent transition point close to the wing trailing edge, thus reducing the drag[4]. Many theoretical and experimental studies on morphing wings have been developed. These studies began with work on independent aerofoils and have been extended to different airplane configurations, especially UAVs. A broad range of aerodynamic optimisation strategies have already been adopted into airplane design.

Recently, morphing wing system studies have branched out into new research directions. Developments in the smart materials field have spurred research on morphing wings, considering their possible use in the design of intelligent wings. One of the biggest morphing projects is the NASA Aircraft Morphing Program, which focuses on developing smart devices to be used in airframe applications to achieve significant improvements in aircraft efficiency and affordability. As smart materials, shape-memory alloys were used to create shape changes in a wing[5]. Many academia, such as Virginia Polytechnic, State University, University of Florida, University of Maryland, Texas A&M University, Delft University and Bristol University, are also engaged in research on morphing wings and have developed various experimental models. In order to achieve the optimal outcomes imposed by the aerodynamic studies, the actuation line of the morphing structure must be precisely controlled. Several control strategies have been adopted as complex functions of the morphing structure and of the actuator types in various morphing applications[6-10].

The global technological evolution has led to the increasing complexity of applications developed in industry and in scientific research fields. Therefore, many researchers have focused their efforts on providing simple control algorithms to cope with the increasing complexity of the controlled systems[11]. The main challenge of a control designer is to find a formal way to convert the knowledge and experience of a system operator into a well-designed control algorithm[12]. From another perspective, the control design method should allow full flexibility in the adjustment of the control surface; taking into account that the systems involved in practice are, generally, complex, strongly nonlinear and often with poorly defined dynamics[11]. If a conventional control methodology, based on linear system theory, is used, a linearised model of the nonlinear system should be developed in advance. Because the validity of a linearised model is limited to a range around the operating point, any guarantee of good performance cannot be provided by a controller obtained in this manner. Therefore, to achieve satisfactory control of a complex nonlinear system, a nonlinear controller must be developed[11-14]. From another viewpoint, if it would be difficult to describe the controlled system precisely by conventional mathematical relations, then the design of a controller based on classical analytical methods would be totally impractical[12,14]. With such systems, there is a motivated interest in using a

control designed by a skilled operator, based on years of experience and knowledge about the static and dynamic characteristics of the system; the controller is known as a fuzzy logic controller (FLC)[14]. FLCs are based on fuzzy logic theory, developed by L. Zadeh[15]. By using multivalent fuzzy logic, linguistic expressions in antecedent and consequent parts of IF-THEN rules describing the operator's actions can be efficiently converted into a fully-structured control algorithm suitable for microcomputer implementation or implementation with specially designed fuzzy processors[12]. In contrast with traditional linear and nonlinear control theory, an FLC is not based on a mathematical model, and it provides a certain level of artificial intelligence to the conventional PID controllers[11].

Some of the most important applications of the fuzzy logic theories in the aerospace field include: the performance of both stability augmentation and automatic flight control functions for the longitudinal and lateral-directional motions for an X-29 aircraft[16], the development of a pitch attitude hold system for a typical fighter jet under a variety of performance conditions that include approach, subsonic cruise and supersonic cruise[17], the design of a flight control system and navigation tasks for autonomous unmanned aerial vehicles[18], the development of an intelligent anti-lock braking system (ABS) control for an aircraft[19,20], the development of an augmented flight control for an F-16 aircraft[21], and the representation, manipulation and utilisation of aerodynamic characteristics in order to model an aircraft with and without winglets[22]. Another application was implemented in a new method for aerodynamic forces conversion from a frequency to a Laplace domain, which was validated on the F/A-18 aircraft for aeroservoelasticity studies[23]. The F/A-18 aircraft non-linear model was identified from flight flutter tests by use of fuzzy logic[24] and a combination of fuzzy logic and neural network methods[25].

This paper presents approaches for the design and validation of a hybrid fuzzy logic proportional-integral-derivative plus conventional on-off controller used in the actuation of a morphing wing. This research work was a part of a large scale morphing wing project, developed with the goal of reducing operating costs for the new generation of aircraft through fuel consumption economy in flight, and also to improve aircraft performance, expanding flight envelopes, replacing conventional control surfaces, reducing drag to improve range and reduce vibrations and flutter. The actuation control concept of the morphing wing uses smart materials such as shape memory alloy (SMA) as actuators. The smart actuators deform dynamically the upper wing surface flexible skin with the aim to delay laminar-to-turbulent flow transition point towards the wing trailing edge[4].

2.0 MORPHING WING PROJECT

The morphing wing research work is a multi-partner project which was mainly funded by the Consortium for Research and Innovation in Aerospace in Quebec (CRIAQ) in collaboration with universities and industries. The project is entitled Laminar Flow Improvement on an Aeroelastic Research Wing, with the main objective to reduce wing form drag by controlling the boundary layer flow behavior on the wing surface. In other words, the wing skin shape is adapting its self automatically to keep the transition point position always close to the wing trailing edge. This project was initiated and funded by aerospace companies Bombardier Aerospace and Thales Avionics, as well as by CRIAQ and the Natural Sciences and Engineering Research Council of Canada (NSERC), and developed by the Ecole de Technologie Supérieure in Montréal (ETS) and the Ecole Polytechnique in Montréal (EP) in collaboration with the Institute for Aerospace Research at the National Research Council Canada (IAR-NRC).

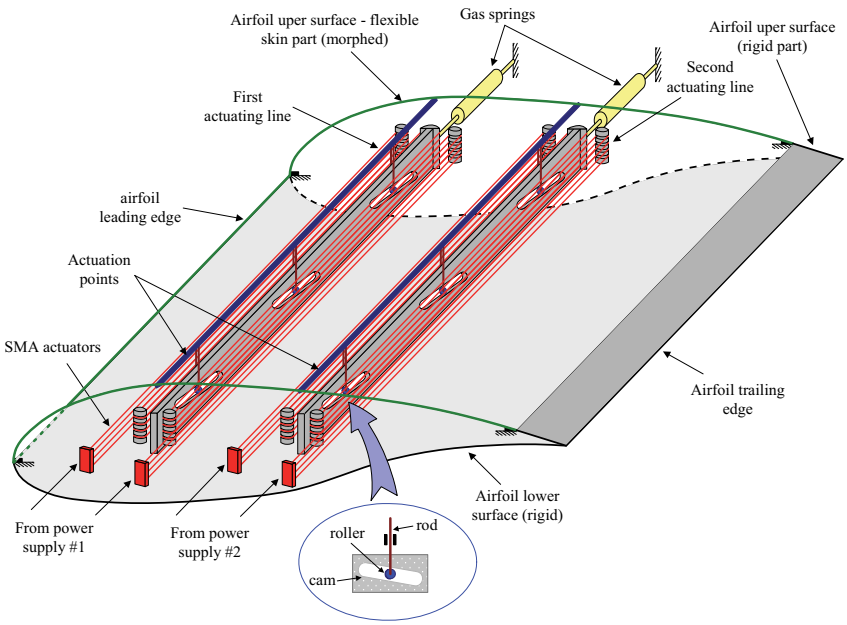

Figure 1. Morphing wing model.

The objectives of the project achieved by ETS Research Laboratory in Active Controls, Avionics and Aeroservoelasticity (LARCASE) were to develop a system for the active control of a morphing wing during flight to maintain large laminar flow run over the upper surface of the wing, and to detect the surface airflow behaviour using pressure sensors installed on the wing skin surface. To this end, numerical simulations and experimental multidisciplinary studies via bench tests and wind tunnel measurements were performed for a morphing wing equipped with a flexible skin, SMA smart material actuators and pressure sensors. Over the course of this research project, investigations were realised on: optical and Kulite sensors' selection and testing for laminar to turbulent flow transition validation (by use of XFoil code and Matlab); smart material actuators' controller methods; aero-elasticity wing studies using MSC/Nastran; open loop and closed loop transition delay controller design; integration and validation on the wing equipped with SMA smart material actuators and pressure sensors (simulation versus test results)[4,26-29]. A thorough validation exercise was performed by comparing the predicting results to the experimental bench and wind tunnel data.

The work described here was developed in the open loop phase of the morphing wing system. The wing model considered was a rectangular plan form wing (0·54m × 0·9m), based on the WTEA-TE1 reference aerofoil (Fig. 1). The lower part of the mechanical model is an aluminium block designed to allow space for the wiring, while the upper part has an aluminium structure equipped with a flexible skin made of composite materials (layers of carbon and Kevlar fibres in a resin matrix) and with the actuation system (shape memory actuators (Ni-Ti)). A number of 35 flow conditions were established as a combination of five Mach numbers (0·2, 0·225, 0·25, 0·275, 0·3) and seven incidence angles (–1˚, –0·5˚, 0˚, 0·5˚, 1˚, 1·5˚, 2˚) to test the morphed structure. Thus, starting from the reference aerofoil, 35 optimised aerofoils were designed based on the flow conditions, with respect the transition location[30].

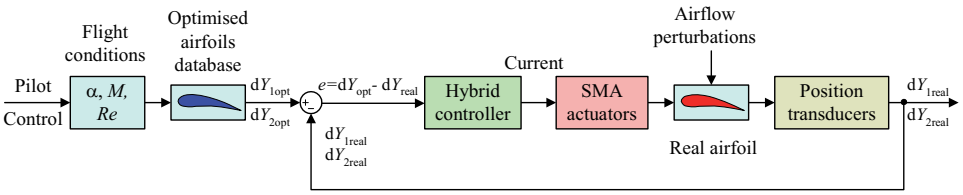

Figure 2. Block diagram of the open loop controlled morphing wing system.

From the initial studies related to the optimal configuration of the flexible structure, two actuation lines, positioned at 25·3% and 47·6% of the chord, from the aerofoil leading edge, were chosen to morph the flexible skin[31-34]. In order to achieve an optimised aerofoil shape for theoretical flow conditions, the flexible skin was required to morph its shape through two actuation points. Two shape memory alloy actuators, of non-linear behaviour, drove the displacement (dY_1, dY_2) of the two control points of the flexible skin towards the optimised aerofoil shape. Each of the shape memory actuators was activated by a power supply unit and were controlled so as to morph the flexible skin until the obtained (real) displacements (dY_{1real}, dY_{2real}) become equal with the desired (optimal) displacements (dY_{1opt}, dY_{2opt}), calculated as differences between the optimised aerofoils and the reference aerofoil at the control points level. The real deflections of the morphed structure were monitored using two position transducers.

3.0 HYBRID CONTROLLER PURPOSES

A block diagram of the open loop controlled morphing wing system, based on the previous considerations, is shown in Fig. 2.

SMA actuator control can be achieved using any method of position control; however, the specific properties of the SMA actuators, such as hysteresis, the first cycle effect and the impact of long-term changes, must be considered. At the same time, the realistic requirements of our system displacements must also be considered.

SMA wires can process the deflections obtained using the applied forces and provide a variety of shapes and sizes that are extremely useful to achieve actuation system goals. For example, SMA wires can provide high forces corresponding to small strains to achieve the right balance between the forces and the deformations, as required by the actuation system. To ensure a stable system, a compromise or balance must be established and maintained. The structural components of the actuation system should be designed to respect the actuators' capabilities to reliably obtain the required deflections and forces.

Despite their simplistic design and mechanical performance, SMAs have their disadvantages. They require a high current to heat rapidly rise their temperature to the material lattice transformation and maintain the current to withstand the displacement. This is translated directly to a significant amount of energy waist. Their volumes are maintained during the entire transformation process; their lengths decrease while their diameters increase. There are also other problems with their attachment to other structures. The wires cannot be directly soldered or epoxied to a surface, as after several cycles of operation, the attachment would be broken. Another issue is that the wire's reliability decreases when over-heated or over-strained. Overheating or over-straining reduced considerably the number of operation cycles from thousands to only few hundreds. Overall, the SMA actuator's disadvantages were deemed to be very small and manageable compared to the problems associated with the other types of smart actuators.

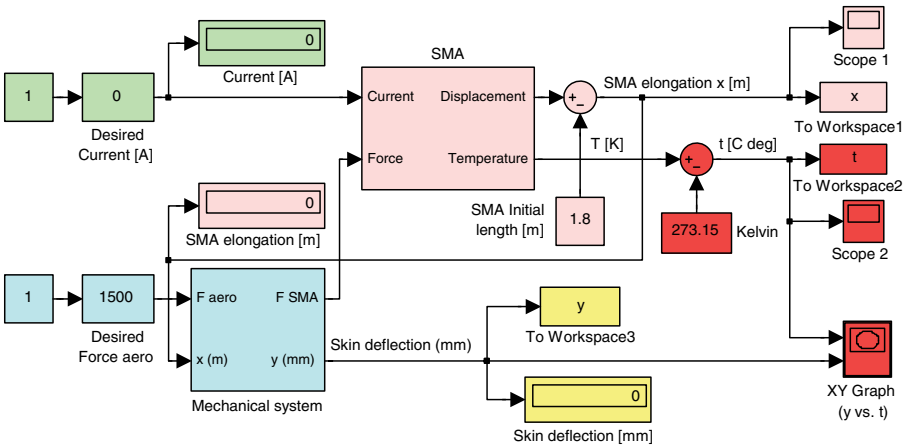

Figure 3. SMA actuators' Matlab/Simulink simulation model.

In the present investigation, each of the actuation lines uses three SMA wires as actuators, and contains a cam, which moves in translation relative to the structure (see Fig. 1). The cam causes the rod motion related to the roller and the skin. A compression gas spring is also used as recall. When the SMA is heated the actuator contracts and the cam moves to the right, resulting in the rise of the roller and the displacement of the skin upwards. Cooling of the SMA, results in a cam motion to the left, and thus a movement of the skin downwards. The horizontal displacement of each actuator is converted into a vertical displacement at a rate of 3:1, which gives the conversion of the horizontal stroke of x mm into a vertical stroke $y = x/3$. From the optimised aerofoils, an approximately 8mm maximum vertical displacement is obtained for the rods, which requires a maximum horizontal displacement of 24mm for the actuators.

In the literature, the modeling and control of smart material actuators are relatively recent research fields[35-40]. Technical literature is available in three independent domains: modeling, control, and smart materials. A smart actuator is formulated for a large range of smart materials and devices, and can be found in a variety of different configurations. It is common knowledge that all physical systems, including smart actuators, contain nonlinearities. As a consequence, smart material actuators can be linearly modelled and may contain errors, while they can also be non-linearly modeled.

The non-linear model used to design and numerically simulate the controller is based on finite element method; the model was built in the Shape Memory Alloys and Intelligent Systems Laboratory (LAMSI) at ETS, using Lickhatchev's theoretical model[41]. The inputs of the SMA model are the alloy initial temperature, the electrical current and the applied force. The outputs are the actuator displacement and the alloy temperature during its functioning. To use the SMA shape-changing characteristics, an initialisation by an external force is required, which obliges it to pass first through the transformation phase and then to return it to the initial phase after the cooling phase. The control could not be realised, due to the intrinsic behaviour of the SMA[29,41].

The simulation model shown in Fig. 3 was obtained by implementing the SMA actuator model using a Matlab *S*-function. To control the SMA actuators, they need to be supplied with an adequate electrical current. The length of the SMA wires is a complex function of the SMA load forces and temperatures, the latter factor being influenced by the supplying current over time

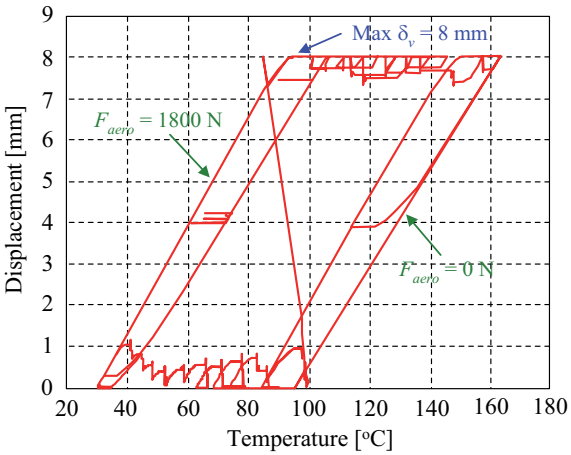

Figure 4. SMA actuator simulated envelope.

and by the interaction of the wires with the environment in the cooling phase (when the electrical supply is switched off)[26,27]. The 'Mechanical system' block considers the forces influencing the SMA load force: the aerodynamic force F_{aero}, the skin force F_{skin}, and the gas spring force F_{spring}.

The envelope of the SMA actuator 1 or 2, obtained through numerical simulations for different aerodynamic load cases, is shown in Fig. 4, where the SMA initial wire length is equal to 1·8m. As can be observed in Fig. 4, to obtain a skin maximum vertical displacement (8mm) in the absence of aerodynamic forces, a high temperature, of approximately 162˚C, is needed to counteract the spring force. Since the ability of the SMA wires to contract is dependent upon Joule heating to produce the required transformation temperature, the need for a higher temperature is reflected by a need for higher electrical current. Also, the envelope in Fig. 4 confirms the strong nonlinear character of the SMA actuator as a function of the load force and temperature.

As shown in Fig. 2, the hybrid controller's purpose is to control the SMA actuators by means of the electrical current supply, in order to cancel the deviation e between the required values for vertical displacements (corresponding to the optimised aerofoils) and the real values, obtained from position transducers. As mentioned previously, the design of such a controller is difficult due to the strong nonlinearities of the SMA actuators' characteristics; these nonlinearities are significantly influenced by the stressing forces. Given these conditions, and considering our research team's experience in fuzzy logic control systems design as well as in SMA modeling, it was decided that one variant of control would be developed with fuzzy logic. On the other hand, because it is normal that in the SMA cooling phase the actuators would not be powered, we adopt a combination of a bi-positional (particularly an on-off one) and a fuzzy logic controller (FLC) for our morphing wing application. This cooling phase may occur not only when controlling a long-term phase, when a switch between two values of the actuator displacements is commended, but also in a short-lived phase, which happens when the real value of the deformation exceeds its desired value and the actuator wires need to be cooled. As a consequence, the hybrid controller should behave as a switch between the SMA cooling and heating phases, in which the output current is 0A, or is controlled by the FLC.

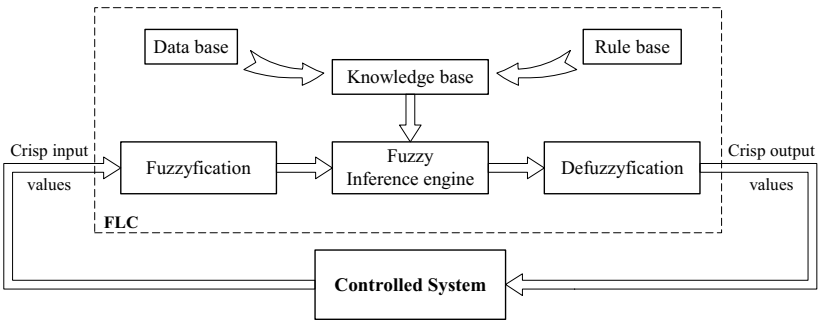

Figure 5. Block diagram of the FLC.

4.0 HYBRID CONTROLLER DESIGN

4.1 FLC structure

Fuzzy logic is an innovative technology that provides tool to interpret the human experience into reality, which enhances conventional system design with engineering expertise. The use of fuzzy logic can help to circumvent the need for rigorous mathematical modeling, which is a very difficult if not an impossible task. Fuzzy logic controllers are rule-based controllers. The basic configuration of a fuzzy logic model can be represented in four parts, as shown in Fig. 5: the fuzzifier, the inference engine, the defuzzifier, and a knowledge base. The fuzzifier reads, measures, scales the control variable, and transforms the measured numerical values to the corresponding linguistic variables with appropriate membership values. The knowledge base includes the definitions of the fuzzy membership functions defined for each control variable and the required (IF-THEN) rules that specify the control goals using linguistic variables. The inference engine calls the fuzzy rule base to derive the linguistic values for the output linguistic variables. The defuzzifier converts the inferred decision from the linguistic variables back to the numerical values. The development of a control system based on fuzzy logic thus involves the following steps: fuzzification strategy, data base building, rule base elaboration, inference machine elaboration and defuzzification strategy[42,43].

The simplest fuzzy logic controller is the proportional controller (*FP*), appropriate for a state or an output feedback in a state space controller. Its input is the error and the output is the control signal. From another perspective, derivative action helps to predict the error, and the proportional-derivative (*PD*) controller makes further use of the derivative action to improve closed-loop stability[44]. The equation of a *PD* controller can be expressed as follows:

$$i(t) = K_P \cdot e(t) + K_D \cdot \frac{\mathrm{d}e(t)}{\mathrm{d}t} = K_P \cdot \left[e(t) + T_D \cdot \frac{\mathrm{d}e(t)}{\mathrm{d}t} \right], \qquad \ldots (1)$$

where $i(t)$ is the command variable (electrical current in the present case), and is time dependent; e is the operating error (see Fig. 2), K_P is the proportional gain and K_D is the derivative gain. The control signal is thus proportional to an estimate of the error T_D seconds ahead, where the estimate is obtained by linear extrapolation. If the T_D time constant is zero, the controller becomes

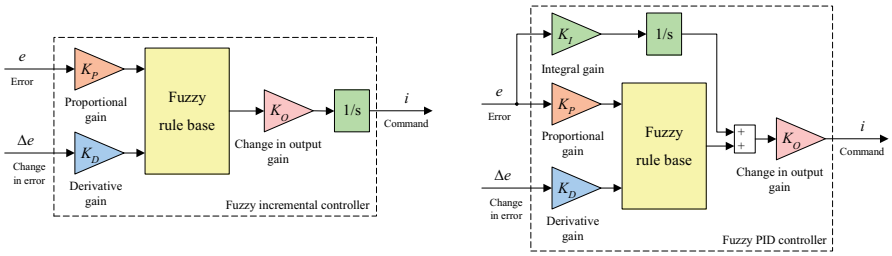

(a) (b)

Figure 6. Fuzzy controller architectures.

a purely proportional one. The gradual increase of the T_D value will produce damped oscillations of the system; over a threshold value the system becomes overdamped[44].

In discrete form, Equation (1) becomes[45]:

$$i(k) = K_P \cdot e(k) + K_D \cdot \Delta e(k), \quad \ldots (2)$$

or

$$i(k) = K_P \cdot e(k) + K_D \cdot \frac{[e(k) - e(k-1)]}{T_S}, \quad \ldots (3)$$

where k is the discrete step, T_s is the sample period and $\Delta e(k)$ is the change in error. Therefore, the inputs to the fuzzy proportional-derivative (FPD) controller are the error and its derivative (called change in error in fuzzy control language).

Additionally, if there is a sustained steady state error, integral action is absolutely necessary[44]. Considering the equation of a proportional-integral (*PI*) controller is easier to find from its discrete form that for a fuzzy *PI* controller obtaining are also used the error and change in error as inputs for the rule base[45]. Literature review has indicated that it is rather difficult to write rules for the integral action, because the integrator windup problem appears due to the physical limitations of the actuator; after the saturation, the control action stays constant, but the error continues to be integrated and the integrator winds up[44].

Two methods to obtain a fuzzy controller with an integral component and avoid the integrator windup problem are proposed in[44]: a fuzzy incremental controller architecture (Fig. 6(a)) and a parallel integral action with a fuzzy PD architecture (Fig. 6(b)). Kumar, Rana, and Gupta[45] give two equivalent architectures for a fuzzy PID controller: (a) fuzzy PI + fuzzy PD in feedback mode and (b) fuzzy PI + fuzzy *PD* in cascade configuration.

The incremental controller (see Fig. 6(a)) has a disadvantage in that it does not include the derivative component well[44]. To take advantage of all the benefits of a PID controller, the structure shown in Fig. 6(b) for our FLC is chosen.

4.2 Input-output mapping

As mentioned above, the output error (e) and the change in error (Δe) are used as controller inputs, and the electrical current i is used as the command variable (controller output). Each of the FLC input or output signals have the real line as the universe of discourse. In practice, the

universe of discourse is restricted to a comparatively small interval; many authors and several commercial controllers use standard universes such as [–1, 1], or [–100, 100] corresponding to percentages of full scale. The universe of discourse of each fuzzy variable can be quantised into a number of overlapping fuzzy sets (linguistic variables). Each element in the universe of discourse is a member of a fuzzy set to some degree; the degree of membership for all its members describes a fuzzy set. The membership function (*mf*) ties a number to each element of the universe. Before designing the membership functions, it is absolutely necessary to consider the universes for the inputs and outputs[42-44].

For our system, the [–1, 1] interval was chosen as the universe for all of the input and output signals. Also, following numerical simulations, we chose three membership functions for each of the two inputs, and five membership functions for the output. The shapes chosen for the input membership functions were the *s*-function, *z*-function, and π-function. Generally, an *s*-function shaped membership function can be implemented using a cosine function:

$$s(x_{left}, x_{right}, x) = \begin{cases} 0, & \text{if } x < x_{left} \\ \frac{1}{2}\left[1 + \text{Cos}\left(\frac{x - x_{right}}{x_{right} - x_{left}}\pi\right)\right], & \text{if } x_{left} \le x \le x_{right}, \\ 1, & \text{if } x > x_{right} \end{cases} \quad \ldots (4)$$

a *z*-function shaped membership function is a reflection of a shaped *s*-function:

$$z(x_{left}, x_{right}, x) = \begin{cases} 1, & \text{if } x < x_{left} \\ \frac{1}{2}\left[1 + \text{Cos}\left(\frac{x - x_{left}}{x_{right} - x_{left}}\pi\right)\right], & \text{if } x_{left} \le x \le x_{right}, \\ 0, & \text{if } x > x_{right} \end{cases} \quad \ldots (5)$$

and a π-function shaped membership function is a combination of both functions:

$$\pi(x_{left}, x_{m1}, x_{m2}, x_{right}, x) = \min[s(x_{left1}, x_{m1}, x),\ z(x_{m2}, x_{right}, x)], \quad \ldots (6)$$

with the peak flat over the $[x_{m1}, x_{m2}]$ middle interval. x is the independent variable on the universe, x_{left} is the left breakpoint, and x_{right} is the right breakpoint[44].

To define the rules, a Sugeno fuzzy model proposed by Takagi, Sugeno and Kang[46] was selected. A Takagi, Sugeno and Kang fuzzy rule for a two input-single output system can be written in the following form:

$$\text{if } (x_1 \text{ is } A) \text{ and } (x_2 \text{ is } B) \text{ then } y = f(x_1, x_2) \quad \ldots (7)$$

where A and B are fuzzy sets in the antecedent, $x = f(x_1, x_2)$ is a crisp function in the consequent, and $f(x_1, x_2)$ is a polynomial function. If f is a constant, then the resulting fuzzy inference is called a zero-order Sugeno fuzzy model. For a two input-single output system, a zero-order Sugeno fuzzy model with N rules is given by[46]:

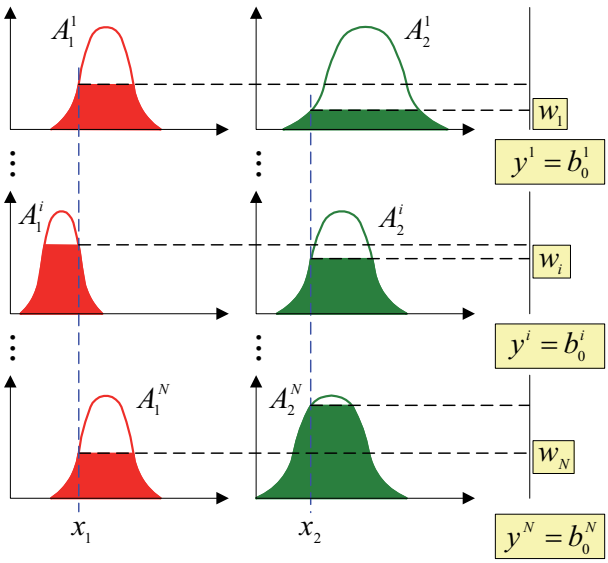

Figure 7. Output of the fuzzy model.

$$\begin{aligned}
&\text{Rule 1: If } x_1 \text{ is } A_1^1 \text{ and } x_2 \text{ is } A_2^1, \text{ then } y^1(x_1,x_2) = b_0^1,\\
&\text{Rule } i\text{: If } x_1 \text{ is } A_1^i \text{ and } x_2 \text{ is } A_2^i, \text{ then } y^i(x_1,x_2) = b_0^i,\\
&\text{Rule } N\text{: If } x_1 \text{ is } A_1^N \text{ and } x_2 \text{ is } A_2^N, \text{ then } y^N(x_1,x_2) = b_0^N,
\end{aligned} \quad \ldots (8)$$

where $x_q (q = \overline{1,2})$ are the individual input variables, $y^i (i = \overline{1,N})$ is the zero-order polynomial function in the consequent, and $A_q^i (i = \overline{1,N})$ are the associated individual antecedent fuzzy sets of each input variable. The coefficients $b_0^i (i = \overline{1,N})$ denote scalar offsets.

For any input vector, $x = [x_1, x_2]^T$, if the singleton fuzzifier, the product fuzzy inference and the center average defuzzifier are applied (Sugeno type), then the output of the fuzzy model y is inferred as follows (weighted average) and shown in Fig. 7:

$$y = \left(\sum_{i=1}^{N} w^i(\mathbf{x}) y^i \right) / \left(\sum_{i=1}^{N} w^i(\mathbf{x}) \right). \quad \ldots (9)$$

$$w^i(\mathbf{x}) = A_1^i(x_1) \times A_2^i(x_2), \quad \ldots (10)$$

which represents the degree of fulfillment of the antecedent, i.e., the level of firing of the i^{th} rule.

In the [–1, 1] universe interval, a three-range partition: negative (*N*), zero (*Z*) and positive (*P*), was chosen for the inputs and , and a five-range partition: negative-big (*NB*), negative-small (*NS*), zero (*Z*), positive-small (*PS*) and positive-big (*PB*) was used for the output. According to the values in Table 1, the membership functions for both inputs are in the form depicted in Fig. 8, and are given by Equations (4), (5) or (6) as:

$$A_1^1(x) = A_2^1(x) = z(-1, 0, x), \quad \ldots (11)$$

Table 1
Parameters of the inputs' membership functions

	***mf* type**	***mf* parameters**			
		x_{left}	x_{m1}	x_{m2}	x_{right}
*mf*1 (A_1^1 and A_2^1)	*z*-function	–1	-	-	0
*mf*2 (A_1^2 and A_2^2)	π-function	–1	0	0	1
*mf*3 (A_1^3 and A_2^3)	*s*-function	0	-	-	1

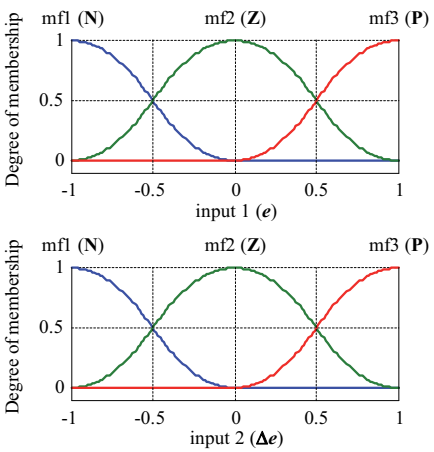

Rule table of the FLC

Δe / e	**N**	**Z**	**P**
N	NB (-1)	NS (-0.5)	Z (0)
Z	NS (-0.5)	Z (0)	PS (0.5)
P	Z (0)	PS (0.5)	PB (1)

Figure 8. Membership functions and rule-based inference for the fuzzy logic controller.

$$A_1^2(x) = A_2^2(x) = \min[s(-1,0,x),\ z(0,1,x)], \quad \ldots (12)$$

$$A_1^3(x) = A_2^3(x) = s(0,1,x), \quad \ldots (13)$$

For the output membership functions, constant values were chosen: $NB = -1$, $NS = -0{\cdot}5$, $Z = 0$, $PS = 0{\cdot}5$, $PB = 1$. Starting from the inputs' and output's membership functions, a set of nine inference rules were obtained ($N = 9$):

$$\begin{aligned}
&\text{Rule 1: If } e \text{ is } A_1^1 \text{ and } \Delta e \text{ is } A_2^1, \text{ then } y^1(e,\Delta e) = -1,\\
&\text{Rule 2: If } e \text{ is } A_1^1 \text{ and } \Delta e \text{ is } A_2^2, \text{ then } y^2(e,\Delta e) = -0.5,\\
&\text{Rule 3: If } e \text{ is } A_1^1 \text{ and } \Delta e \text{ is } A_2^3, \text{ then } y^3(e,\Delta e) = 0,\\
&\text{Rule 4: If } e \text{ is } A_1^2 \text{ and } \Delta e \text{ is } A_2^1, \text{ then } y^4(e,\Delta e) = -0.5,\\
&\text{Rule 5: If } e \text{ is } A_1^2 \text{ and } \Delta e \text{ is } A_2^2, \text{ then } y^5(e,\Delta e) = 0,\\
&\text{Rule 6: If } e \text{ is } A_1^2 \text{ and } \Delta e \text{ is } A_2^3, \text{ then } y^6(e,\Delta e) = 0.5,\\
&\text{Rule 7: If } e \text{ is } A_1^3 \text{ and } \Delta e \text{ is } A_2^1, \text{ then } y^7(e,\Delta e) = 0,\\
&\text{Rule 8: If } e \text{ is } A_1^3 \text{ and } \Delta e \text{ is } A_2^2, \text{ then } y^8(e,\Delta e) = 0.5,\\
&\text{Rule 9: If } e \text{ is } A_1^3 \text{ and } \Delta e \text{ is } A_2^3, \text{ then } y^9(e,\Delta e) = 1.
\end{aligned} \quad \ldots (14)$$

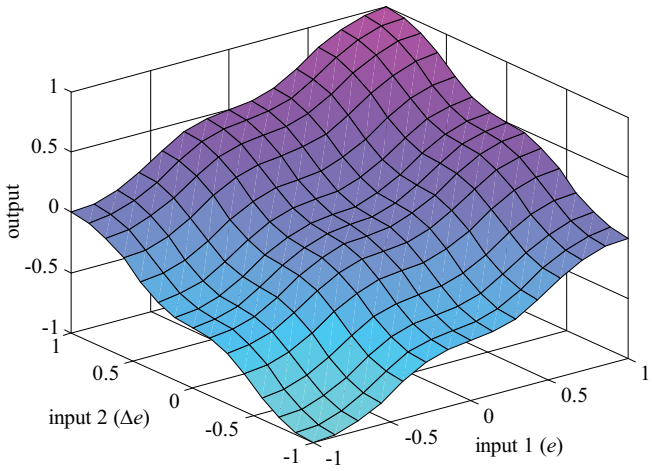

Figure 9. The fuzzy control surface.

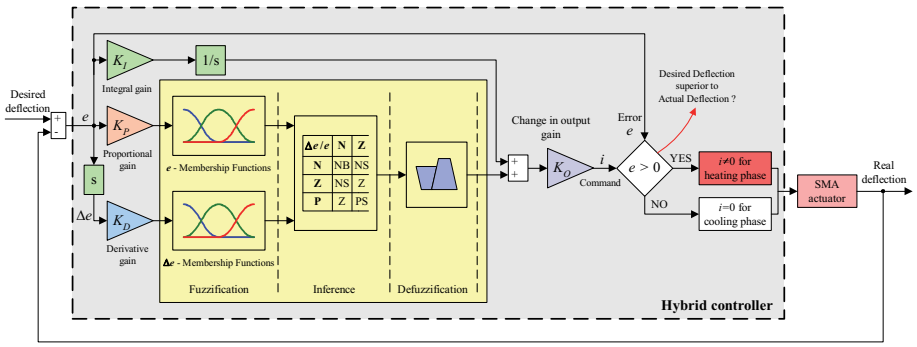

Figure 10. Hybrid controller architecture.

The rule-based inference chosen for each consequent is also presented in Fig. 8. With the previous considerations, the fuzzy control surface results in the form presented in Fig. 9.

4.3 Hybrid controller resulted architecture

Starting from the observation that in the SMA cooling phase the actuators are not powered, we have chosen a combination of a bi-positional (particularly an on-off) and a fuzzy logic controller (FLC) for our morphing application. As we have stated earlier, the cooling phase may occur not only when controlling a long-term phase, when a switch between two values of the actuator displacements is ordered, but also in a short-lived phase, which occurs when the real value of the deformation exceeds its desired value. As a consequence of this need and of the previous FLC description, the resulting architecture for the hybrid controller is shown in Fig. 10.

5.0 CONCLUSIONS

The approaches for the design of a hybrid fuzzy logic proportional-integral-derivative plus a conventional on-off controller used in the actuation of a morphing wing were presented. The actuation control concept of the morphing wing uses smart materials such as shape memory Alloy (SMA) as actuators. These smart actuators modify the flexible skin upper wing surface, so that the laminar-to-turbulent transition point moves close to the wing aerofoil trailing edge. The simulated envelope of the SMA actuator confirms that the length of the SMA wires is a complex nonlinear function of the SMA load force and temperature, the latter influenced by the supplying current over time and by the interaction of the wires with the environment in their cooling phase (when the electrical supply is removed).

To achieve the aerodynamic goal for the morphing wing (moving the laminar-to-turbulent transition point close to the wing aerofoil trailing edge), a first phase of studies involved the determination of optimised aerofoils available for 35 different flow conditions (combinations of five Mach numbers and seven angles-of-attack). The hybrid controller's purpose was the control of the SMA actuators by means of the electrical current supply, with the aim of canceling the deviations between the required values for vertical displacements (corresponding to the optimised aerofoils) and the real experimental values, obtained from position transducers. Because of the strong nonlinearities of the SMA actuators' characteristics (nonlinearities that are significantly influenced by the forces employed to tense them), a fuzzy logic control variant was developed. In addition, because it is normal that the actuators are not powered in the SMA cooling phase, a combination of a bi-positional (particularly an on-off) and a fuzzy logic controller was chosen. The hybrid controller behaved as a switch between the SMA cooling and heating phases, in situations where the output current was 0 *A*, or it was controlled by the fuzzy logic controller. The fuzzy logic controller scheme chosen was a proportional-integral-derivative. The shapes chosen for the input membership functions were the *s*-function, π-function, and *z*-function, and product fuzzy inference and the Sugeno center-average defuzzifier were applied.

After this preliminary design step, a complete validation cycle of the hybrid controller was realised (numerical simulations, experimental bench test in laboratory conditions without aerodynamic force loads, and a final wind tunnel test) and will be presented in the second part of this paper.

ACKNOWLEDGEMENTS

The authors would like to thank the Consortium for Research and Innovation in Aerospace in Quebec (CRIAQ), Thales Canada and Bombardier Aerospace for their financial and technical support. The authors also wish to express their appreciation to Mr George Henri Simon for initiating the CRIAQ 7.1 project and to Mr Philippe Molaret from Thales Canada for their collaboration in this work.

REFERENCES

1. PATEL, S.C., MAJJI, M., KOH, B.S., JUNKINS, J.L. and REDINIOTIS, O.K. Morphing wing: A demonstration of aero servo elastic distributed sensing and control, 2005, Final research paper in 2005 Summer Research Experience for Undergraduates (REU) on Nanotechnology and Materials Systems, Texas Institute of Intelligent Bio-Nano Materials and Structures for Aerospace Vehicles (TiiMS) – NASA Research University, Texas A&M University, July 2005, College Station, TX, USA.

2. GANO, S.E and RENAUD, J.E. Optimized unmanned aerial vehicle with wing morphing for extended range and endurance, 2002, Ninth AIAA/ISSMO Symposium and Exhibition on Multidisciplinary Analysis and Optimization, 4-6 September 2002, Atlanta, GA, USA, pp 1-9.
3. CADOGAN, D., SMITH, T., UHELSKY, F. and MACKUSICK, M. Morphing inflatable wing development for compact package unmanned aerial vehicles, 2004, 45th AIAA/ASME/ASCE/AHS/ASC Structures, Structural Dynamics and Materials Conference, 19-22 April 2004, Palm Springs, CA, USA.
4. POPOV, A.-V., BOTEZ, R.M., MAMOU, M., MEBARKI, Y., JAHRHAUS, B., KHALID. M. and GRIGORIE, T.L. Drag reduction by improving laminar flows past morphing configurations, 2009, AVT-168 NATO Symposium on the Morphing Vehicles, 20-23 April 2009, Evora, Portugal.
5. WLEZIEN, R.W., HORNER, G.C., MCGOWAN, A.R., PADULA, S.L., SCOTT, M.A., SILCOX, R.J. and SIMPSON, J.O. The aircraft morphing program, AIAA-1998-1927.
6. BLISS, T.K. and BART-SMITH, H. Morphing structures technology and its application to flight control, 2005, Student Research Conference, Virginia Space Grant Consortium, 1 April 2005, Newport News, VA, USA.
7. WHITMER, C.E and KELKAR, A.G. Robust control of a morphing airfoil structure, 2005, American Control Conference, 8-10 June 2005, Portland, OR, USA.
8. RUOTSALAINEN, P., NEVALA, P.K., BRANDER, T., LINDROOS, T. and SIPPOLA, M. Shape control of a FRP airfoil structure using SMA-actuators and optical fiber sensors, *J Solid State Phenomena*, 2009, **144**, Mechatronic Systems and Materials II, pp 196-201.
9. LAMPTON, A., NIKSCH, A. and VALASEK, J. Reinforcement learning of a morphing airfoil-policy and discrete learning analysis, 2008, AIAA Guidance, Navigation and Control Conference and Exhibition, 18-21 August 2008, Honolulu, Hawaii, USA.
10. LAMPTON, A., NIKSCH, A. and VALASEK, J. Morphing airfoils with four morphing parameters, 2008, AIAA Guidance, Navigation and Control Conference and Exhibition, 18-21 August 2008, Honolulu, Hawaii, USA.
11. AL-ODIENAT, A.I. and AL-LAWAMA, A.A. The advantages of PID fuzzy controllers over the conventional types, *American J Applied Sciences*, 2008, **5**, (6), pp 653-658.
12. KOVACIC, Z. AND BOGDAN, S. *Fuzzy Controller Design – Theory and Applications*, 2006, Taylor and Francis Group.
13. VERBRUGGEN, H.B. and BRUIJN, P.M. Fuzzy control and conventional control: What is (and can be) the real contribution of fuzzy systems?, *Fuzzy Sets Systems*, September 1997, **90**, (2), pp 151–160.
14. HAMPEL, R., WAGENKNECHT, M. and CHAKER, N. Fuzzy control – Theory and practice, *Physica-Verlag*, 2000.
15. ZADEH, L.A. Fuzzy sets, *Information Control*, 1965, **8**, pp 339-353.
16. LUO, J. and LAN, E. *Fuzzy Logic and Intelligent Systems – Fuzzy Logic Controllers for Aircraft Flight Control*, 7 July 2007, pp 85-124, Springer.
17. VICK, A. and COHEN, K. Longitudinal stability augmentation using a fuzzy logic based PID controller, 2009, Fuzzy Information Processing Society, 2009, NAFIPS 2009, Annual Meeting of the North American, 14-17 June 2009, pp 1-6.
18. KURNAZ, S., CETIN, O. and KAYNAK, O. Fuzzy logic based approach to design of flight control and navigation tasks for autonomous unmanned aerial vehicles, *J Intelligent and Robotic Systems*, 2009, **54**, pp 229–244
19. URSU, I. and URSU, F. An intelligent ABS control based on fuzzy logic. Aircraft application, 2003, Proceedings of the International Conference on Theory and Applications of Mathematics and Informatics – ICTAMI, 2003, Alba Iulia, Romania, pp 355-368.
20. URSU, I. and URSU, F. Airplane ABS control synthesis using fuzzy logic, *J Intelligent & Fuzzy Systems: Applications in Engineering and Technology*, January 2005, **16**, (1), pp 23-32.
21. STEWART, P., GLADWIN, D., PARR, M. and STEWART, J. Multi-objective evolutionary–fuzzy augmented flight control for an F16 aircraft, 2010, Proceedings of the Institution of Mechanical Engineers, Part G, *J Aerospace Engineering*, 1 March 2010, **224**, (3), pp 293-309.
22. HOSSAIN, A., RAHMAN, A., HOSSEN, J., IQBAL, A.K.M.P. and HASAN, S.K. Application of fuzzy logic approach for an aircraft model with and without winglet, *Int J Mechanical, Industrial and Aerospace Eng*, 2010, **4**, (2), pp 78-86.
23. HILIUTA, A., BOTEZ, R.M. and BRENNER, M. Approximation of unsteady aerodynamic forces Q, k, M by use of fuzzy techniques. *AIAA J*, 2005, **43**, (10), pp 2093–2099.

24. KOUBA, G., BOTEZ, R.M. and BOELY, N. Identification of F/A-18 model from flight tests using the fuzzy logic method, 2009, 47th AIAA Aerospace Sciences Meeting, 5-8 January 2009, Orlando, FL, USA.
25. BOELY, N., BOTEZ, R.M. and KOUBA,G. Identification of an F/A-18 nonlinear model between control and structural deflections, 2009, 47th AIAA Aerospace Sciences Meeting, 5–8 January 2009, Orlando, FL, USA.
26. GRIGORIE, L.T. and BOTEZ, R.M. New adaptive controller method for SMA hysteresis modelling of a morphing wing, *Aeronaut J*, January 2010, **114**, (1151), pp 1-13.
27. GRIGORIE, L.T. and BOTEZ, R.M. Adaptive neuro-fuzzy inference system based controllers for smart material actuator modeling, *J Aerospace Eng*, 2009, **223**, (G6), pp 655-668.
28. POPOV, A-V., BOTEZ, R. M., MAMOU, M. and GRIGORIE, T.L. Optical sensor pressure measurements variations with temperature in wind tunnel testing, *AIAA J Aircr*, 2009, **46**, (4), pp 1314-1318.
29. POPOV. A-V., LABIB, M., FAYS, J. and BOTEZ, R.M. Closed loop control simulations on a morphing laminar airfoil using shape memory alloys actuators, *AIAA J Aircr*, 2008, **45**, (5), pp 1794-1803.
30. SAINMONT, C., PARASCHIVOIU, I. and COUTU, D. Multidisciplinary approach for the optimization of a laminar airfoil equipped with a morphing upper surface, 2009, NATO AVT-168 Symposium on 'Morphing Vehicule', Evora, Portugal.
31. GEORGES, T., BRAILOVSKI, V., MORELLON, E., COUTU, D. and TERRIAULT, P. Design of shape memory alloy actuators for morphing laminar wing with flexible extrados, *J Mechanical Design*, September 2009, **31**, (9), 091006.
32. BRAILOVSKI, V., TERRIAULT, P., COUTU, D., GEORGES, T., MORELLON, E., FISCHER, C. and BERUBE, S. Morphing laminar wing with flexible extrados powered by shape memory alloy actuators, 2008, ASME Conference Smart Materials, Adaptive Structures and Intelligent Systems (SMASIS), Paper 337, Ellicott City, USA.
33. COUTU, D., BRAILOVSKI, V., TERRIAULT, P. and FISCHER, C. Experimental validation of the 3D numerical model for an adaptive laminar wing with flexible extrados, 2007, 18th International Conference of Adaptive Structures and Technologies, 3-5 October 2007, Ottawa, Ontario, Canada.
34. COUTU, D., BRAILOVSKI, V. and TERRIAULT, P. Promising benefits of an active-extrados morphing laminar wing, *AIAA J Aircr*, 2009, **46**, (2), pp 730-731.
35. HARTL, D.J. and LAGOUDAS D.C. Aerospace applications of shape memory alloys, Proceedings of the Institution of Mechanical Engineers, Part G: *J Aerospace Eng*, April 2007, **221**, (4), pp 535-552.
36. KHANDELWAL, A. and BURAVALLA, V. Models for shape memory alloy behavior: An overview of modeling approaches, *Int J Structural Changes in Solids – Mechanics and Applications*, December 2009, **1**, (1), pp 111-148.
37. LIU, S.H., HUANG, T.S. and YEN, J.Y. Tracking control of shape-memory-alloy actuators based on self-sensing feedback and inverse hysteresis compensation, *Sensors*, 2010, **10**, pp 112-127.
38. KAPPS, M. Smart-material mechanisms as actuation alternatives for aerospace robotics and automation, 2006, International Space Development Conference, ISDC06, pp 19, 4-7 May 2006, Los Angeles, USA.
39. DUTTA, S.M., GHORBEL, F.H. and DABNEY, J.B. Modeling and control of a shape memory alloy actuator, 2005, IEEE International Symposium on Intelligent Control, pp 1007-1012, 27-29 June 2005, Limassol, Cyprus.
40. DEFARIA, C.T., BORDUQUI, H.G., CAVALINI, A.A. and LOPES, V. Active control position using shape memory alloys, 2009, IMAC-XXVII, 9-12 February 2009, p 8, Orlando, FL, USA.
41. TERRIAULT, P., VIENS, F. and BRAILOVSKI, V. Non-isothermal finite element modeling of a shape memory alloy actuator using ANSYS, *Computational Materials Science*, July 2006, **36**, (4), pp 397-410.
42. TOMESCU, B. On the Use of Fuzzy Logic to Control Paralleled dc-dc Converters, Dissertation, October, 2001, Virginia Polytechnic Institute and State University Blacksburg, VA, USA.
43. CORCAU, J. I. and STOENESCU, E. Fuzzy logic controller as a power system stabilizer, *Int J Circuits, Systems and Signal Processing*, 2007, **3**, (1), pp 266-273.
44. JANTZEN, J. Tuning of fuzzy PID controllers, September 1998, Technical Report 98-H871, Department of Automation, Technical University of Denmark.
45. Kumar, V., Rana, K.P.S. and Gupta, V. Real-time performance evaluation of a fuzzy PI + fuzzy PD controller for liquid-level process, *Int J Intelligent Control and Systems*, June 2008, **13**, (2), pp 89-96.
46. MAHFOUF, M., LINKENS, D. A. and KANDIAH, S. Fuzzy Takagi-Sugeno Kang model predictive control for process engineering, 1999, 4 pp, IEE, London, UK.